

Tricarbonylmanganese(I) and -rhenium(I) Complexes of Imidazol-Based Phosphane Ligands: Influence of the Substitution Pattern on the CO Release Properties

Peter C. Kunz,^{*[a]} Wilhelm Huber,^[a] Alfonso Rojas,^[b] Ulrich Schatzschneider,^[b] and Bernhard Spingler^[c]

Keywords: Manganese / Rhenium / CO-releasing molecules / N ligands / Tripodal ligands

Tricarbonylmanganese(I) and -rhenium(I) complexes of the imidazolylphosphane ligands tris(imidazol-2-yl)phosphane (2-TIP^{Pr}), tris(*N*-methylimidazol-2-yl)phosphane (2-TIP^{NMe}), and tris[2-isopropylimidazol-4(5)-yl]phosphane (4-TIP^{Pr}) as well as the phosphane oxide (4-TIPO^{Pr}) and sulfide (4-TIPS^{Pr}) ligands were prepared. These tris(imidazolyl) ligands act as *N,N,N*-tripodal chelating ligands. The solid-state structures of the manganese complexes [(2-TIP^{NMe})Mn(CO)₃]OTf and [(4-TIPS^{Pr})Mn(CO)₃]OTf as well as the rhenium

compound [(4-TIPO^{Pr})Re(CO)₃]OTf were determined by X-ray diffraction. The potential of these complexes as photoactivatable CO-releasing molecules (CORMs) was studied with the UV/Vis spectroscopy-based myoglobin assay. Within the series of compounds prepared, the substitution pattern of the imidazolyl groups was found to significantly influence the CO-release efficiency and stoichiometry. (© Wiley-VCH Verlag GmbH & Co. KGaA, 69451 Weinheim, Germany, 2009)

Introduction

For a long time, carbon monoxide (CO) was mostly seen as a dangerous air pollutant because of its properties as an odorless and colorless gas that is highly toxic to humans due to its interference with the oxygen transport in blood. In recent years, it has, however, become clear that carbon monoxide is endogenously produced in the human body by tightly controlled enzymatic degradation of heme and serves as an important small-molecule messenger, much like nitric oxide (NO).^[1–3] In addition, deliberate application of CO was found to give rise to a number of beneficial physiological effects because of its antiinflammatory, antioxidative, and antiapoptotic activities. In animal experiments, it was also shown to affect ocular hypertension as well as coagulation processes associated with transplantations.^[4–6]

As CO itself is difficult to dose and is a highly toxic gas, there is currently significant interest in the application of carbonylmetal complexes as a solid “storage form” for car-

bon monoxide. An increasing number of such “CO-releasing molecules” (CORMs) are being studied to optimize their CO-release characteristics and achieve sufficient water solubility for therapeutic applications.^[7–9] Whereas Motterlini et al. have pioneered the use of carbonylruthenium compounds, with tricarbonylchloro(glycinato)ruthenium(II) (CORM-3) as the CO-releasing molecule most commonly employed in biological studies at present,^[10] more recently carbonyl(pyrone)iron and -molybdenum complexes (CORM-F7 and CORM-F10) have also received considerable attention.^[11–13] Whereas in these complexes the CO release is usually triggered by ligand-substitution reactions in aqueous solution, an alternative approach has explored the light-induced liberation of carbon monoxide from dark-stable carbonylmanganese complexes, like [Mn₂(CO)₁₀] (CORM-2).^[14] In particular, the tricarbonyl complex [(tpm)Mn(CO)₃]PF₆ was shown to release CO upon UV radiation and exhibit cytotoxic activity against cancer cells while being inactive even after prolonged exposure in the dark.^[15,16] Although the number of studies on carbonylmetal CORMs has significantly grown over recent years, very few systematic studies of the factors determining the mechanism of CO release have been carried out.^[17,18]

Here, we report on the synthesis and characterization of a series of Mn(CO)₃ and Re(CO)₃ complexes of different imidazol-2-yl and imidazol-4(5)-ylphosphane ligands. Since the introduction of the tris(pyrazolyl)boranes (tp) by Trofimenko, scorpionate ligands containing N-donor atoms have been intensively studied and are well known as ligands for complexes used in biomedical applications.^[19–21] The tris-

[a] Institut für Anorganische Chemie und Strukturchemie I, Heinrich-Heine-Universität Düsseldorf, Universitätsstr. 1, 40225 Düsseldorf, Germany
Fax: +49-211-81-12287
E-mail: peter.kunz@uni-duesseldorf.de

[b] Lehrstuhl für Anorganische Chemie I - Bioanorganische Chemie, Ruhr-Universität Bochum NC 3/74, Universitätsstr. 150, 44801 Bochum, Germany
Fax: +49-234-32-14378
E-mail: ulrich.schatzschneider@rub.de

[c] Anorganisch-Chemisches Institut, Universität Zürich-Irchel, Winterthurerstr. 190, 8057 Zürich, Switzerland

Supporting information for this article is available on the WWW under <http://dx.doi.org/10.1002/ejic.200900650>.

(imidazol-2-yl)phosphanes and tris[imidazol-4(5)-yl]phosphanes used in this study are neutral analogues of the tp ligand in which the hydrolytically unstable B–N bonds have been replaced by more stable P–C bonds.^[22,23] To assess the bioavailability of these new complexes, their stability and distribution coefficient in physiological media have been studied, followed by an investigation of light-induced CO release from the Mn complexes.

Results and Discussion

The imidazol-2-ylphosphanes 2-TIP^H and 2-TIP^{NMe} were prepared according to the procedures reported by Wu et al.^[24] and Brown et al.^[25] The ligands 4-TIP^{*i*Pr}, 4-TIPO^{*i*Pr}, and 4-MIP^{*i*Pr} were synthesized as reported previously.^[22,23,26] For the synthesis of 4-TIPS^{*i*Pr}, the sulfurization reaction was carried out in ethanol under reflux by using 4-TIP^{*i*Pr} and elemental sulfur.

The rhenium complexes **1a–5a** (Figure 1) were prepared by addition of a solution of the corresponding ligand to a solution of [Re(H₂O)₃(CO)₃]Br in methanol.^[27] In this reaction, the phosphane ligand 4-TIP^{*i*Pr} was found to coordinate exclusively in the C_{3v}-symmetric *N,N,N*-binding mode, and compound **3a** was obtained in excellent yield. On the other hand, when 4-TIP^{*i*Pr} was treated with [Re(CO)₅Br] under the same conditions, a mixture of products was obtained, as can be seen in the ³¹P{¹H} NMR spectrum of the reaction mixture. Very likely, the 4-TIP^{*i*Pr} ligand adopts different coordination modes here, which might also involve binding of the phosphorus atom to the metal center. As an example of such a *P*-bound imidazol-4(5)-ylphosphane, we

were able to structurally characterize complex **6** (Figure 1), where two diphenyl[imidazol-4(5)-yl]phosphane ligands (4-MIP^{*i*Pr}) are coordinated to the Re(CO)₃ core. When the phosphorus atom of the 4-TIP^{*i*Pr} is oxidized or modified by sulfurization, however, only the tripodal *N,N,N*-binding mode is possible. Espinet et al. reported on the formation of analogous Mo(CO)₃ complexes of tris(pyridin-2-yl)phosphane (Ppy₃)-based ligands. They found that in the reaction of [Mo(CO)₆] or [Mo(CO)₄(nbd)] (nbd:norbornadiene) with Ppy₃, intermediates form in which the Ppy₃ ligand is *P,N,N*-bound, whereas the final product shows *N,N,N*-coordination.^[28]

Complex **5a** could not be prepared in analytically pure form as it was always found to be contaminated by small amounts of **4a**. Additionally, the presence of hydrogen sulfide could be recognized by its characteristic smell. Obviously, traces of water lead to hydrolysis of the 4-TIPS^{*i*Pr} ligand during the reaction.

The synthesis of manganese complexes **1b–5b** (Figure 1) was straightforward. After in situ preparation of [Mn(CO)₃(solv)₃]OTf by abstraction of the bromide ion from [Mn(CO)₅Br] with silver triflate, the respective ligand was added in acetone to obtain the desired complexes in good yield.

The IR stretching frequencies and chemical shifts of the ³¹P NMR resonances of all complexes are reported in Table 1. All complexes **1–5** show two bands in the carbonyl region typical for C_{3v}-symmetrical compounds. In addition, their ¹H NMR spectra show only one set of signals for the protons of the three equivalent imidazolyl rings. Although the phosphorus atom is not coordinated to the metal center,

Table 1. IR and ³¹P{¹H} NMR spectroscopic data of complexes [LM(CO)₃]⁺ (**1–5**) and [L₂Re(CO)₃Br] (**6**).

L	M	Complex	$\nu(\text{CO})$ [cm ⁻¹]	³¹ P{ ¹ H} δ [ppm]
2-TIP ^H	Re	1a	1922, 2031	-99.2
	Mn	1b	1915, 2042	-101.7
2-TIP ^{NMe}	Re	2a	1886, 2007	-113.5
	Mn	2b	1919, 2033	-115.7
4-TIP ^{<i>i</i>Pr}	Re	3a	1902, 2021	-101.4
	Mn	3b	1933, 2027	-103.6
4-TIPO ^{<i>i</i>Pr}	Re	4a	1914, 2026	+3.0
	Mn	4b	1935, 2031	+1.3
4-TIPS ^{<i>i</i>Pr}	Re	5a	1908, 2029	-3.4
	Mn	5b	1929, 2032	-7.0
4-MIP ^{<i>i</i>Pr}	Re	6	1920, 1948, 2031	-16.1

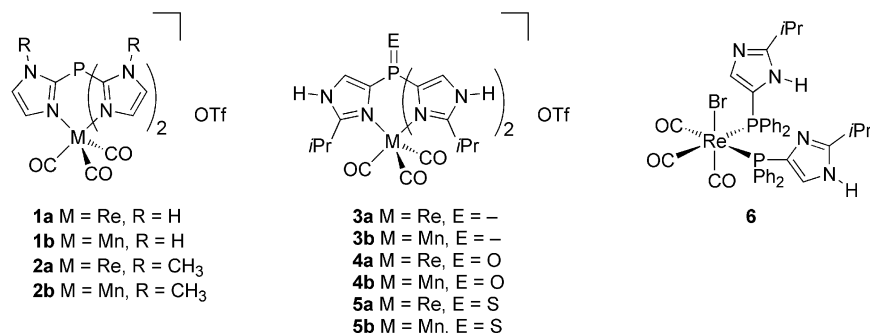


Figure 1. Manganese and rhenium complexes **1–6** investigated in this study.

the $^{31}\text{P}\{^1\text{H}\}$ NMR signal of the P^{III} atoms in **1–3** shifts to higher field by about 25 ppm upon coordination of the ligand to the $\text{M}(\text{CO})_3$ moiety. A similar observation was made by Johnson for ligands of the type $\text{P}(\text{CH}_2\text{-NHR})_3$.^[29–32] The shift of the $^{31}\text{P}\{^1\text{H}\}$ NMR signal of **6**, which is a classical coordination shift, is 15 ppm to a lower field. The ^1H NMR spectrum of bis(ligand) complex **6** shows one set of signals for the two coordinated ligands, and in the IR spectrum three bands typical of a C_3 -symmetrical complex are found.^[33]

Solid-State Structures

Several of the new complexes could be characterized by X-ray structure analysis of suitable single crystals. Complex **2b** crystallizes in the monoclinic space group $P2_1/c$. Crystals were obtained by slow diffusion of diethyl ether into a solution of **2b** in methanol. Alternatively, from a solution of **2b** in acetone, the solvate $\mathbf{2b}\cdot(\text{CH}_3)_2\text{CO}$ was crystallized. In this case, the space group was determined as triclinic $P\bar{1}$. The metrical parameters of the complex cation are identical in both structures, thus only the former structure is shown in Figure 2. The parameters are comparable to those of tris(pyrazolyl)methane (tpm) complexes $[\text{Mn}(\text{CO})_3(\text{tpm})]^+$.^[15,34–38]

Compound **4a** crystallizes with two solvent molecules in the lattice as $\mathbf{4a}\cdot\text{H}_2\text{O}\cdot(\text{CH}_3)_2\text{CO}$ in the triclinic space group $P\bar{1}$ (see Figure 3). The 4-TIPO^{iPr} ligand is coordinated to the rhenium atom in a tripodal N,N,N -fashion. In addition, the Re^{I} center is facially bound to three CO ligands. The metrical parameters are comparable to those of tris(pyrazolyl)methane (tpm) complexes of $\text{Re}(\text{CO})_3$.^[39–42]

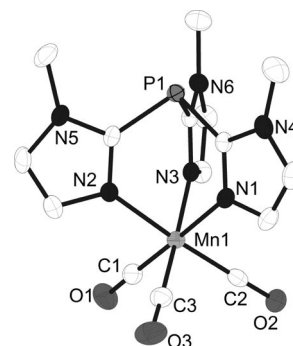


Figure 2. Solid-state structure of **2b**. The counterion and H atoms are omitted for clarity. Displacement ellipsoids are drawn at the 50% level.

Compound **5b** crystallizes with a molecule of diethyl ether in the lattice as $\mathbf{5b}\cdot\text{C}_4\text{H}_{10}\text{O}$ in the orthorhombic space group $Pnma$ (see Figure 4). Cation, anion, and solvate molecules are all dissected by the mirror plane of the space group. As found in the Re^{I} complex **4a**, the Mn^{I} center is also in an octahedral coordination environment, bound to three CO ligands and three nitrogen donor atoms from the facially coordinating 4-TIPS^{iPr} ligand. As for **2b**, the metrical parameters of **5b** are comparable to those of tris(pyrazolyl)methane (tpm) complexes $[\text{Mn}(\text{CO})_3(\text{tpm})]^+$.^[15,34–38] Selected bond lengths and angles of the N,N,N -bound $[\text{LM}(\text{CO})_3]\text{X}$ compounds **2b**, $\mathbf{2b}\cdot(\text{CH}_3)_2\text{CO}$, $\mathbf{4a}\cdot\text{H}_2\text{O}\cdot(\text{CH}_3)_2\text{CO}$, and $\mathbf{5b}\cdot(\text{C}_2\text{H}_5)_2\text{O}$ are summarized in Table 2.

The bis(ligand) complex **6** crystallizes in the monoclinic space group $P2_1/c$. The two imidazolylphosphane ligands are bound to the *fac*- $\text{Re}(\text{CO})_3$ core through their phospho-

Table 2. Selected bond lengths [\AA] and angles [$^\circ$] for the N,N,N -bound $[\text{LM}(\text{CO})_3]\text{X}$ compounds **2b**, $\mathbf{2b}\cdot(\text{CH}_3)_2\text{CO}$, $\mathbf{4a}\cdot\text{H}_2\text{O}\cdot(\text{CH}_3)_2\text{CO}$, and $\mathbf{5b}\cdot(\text{C}_2\text{H}_5)_2\text{O}$.

d [\AA]	2b	$\mathbf{2b}\cdot(\text{CH}_3)_2\text{CO}$	$\mathbf{4a}\cdot\text{H}_2\text{O}\cdot(\text{CH}_3)_2\text{CO}$	$\mathbf{5b}\cdot(\text{C}_2\text{H}_5)_2\text{O}$
M–C(1)	1.792(3)	1.794(3)	1.914(8)	1.808(3)
M–C(2)	1.821(3)	1.802(3)	1.953(8)	1.804(4)
M–C(3)	1.813(3)	1.811(3)	1.943(8)	–
M–N(1)	2.053(2)	2.058(2)	2.226(6)	2.105(2)
M–N(2)	2.062(2)	2.0516(18)	2.211(5)	2.123(3)
M–N(3)	2.069(2)	2.055(2)	2.229(5)	–
C(1)–O(1)	1.149(3)	1.153(3)	1.152(10)	1.144(4)
C(2)–O(2)	1.137(3)	1.151(3)	1.113(10)	1.140(5)
C(3)–O(3)	1.142(3)	1.140(3)	1.132(10)	–
Angle [$^\circ$]				
C(1)–M–C(2)	89.33(12)	89.63(12)	91.9(3)	89.19(12)
C(1)–M–C(3)	89.86(13)	91.58(13)	90.0(3)	92.05(12)
C(2)–M–C(3)	90.87(13)	89.92(12)	92.3(3)	–
N(1)–M–N(2)	86.50(9)	87.05(7)	84.9(2)	88.39(8)
N(1)–M–N(3)	86.88(9)	86.71(7)	86.0(2)	86.71(11)
N(2)–M–N(3)	85.93(9)	85.24(8)	85.1(2)	–
C(1)–M–N(1)	178.11(11)	177.31(11)	175.9(3)	176.99(10)
C(1)–M–N(2)	93.01(11)	90.90(10)	91.5(3)	90.17(10)
C(1)–M–N(3)	91.27(11)	92.90(11)	91.7(3)	90.60(10)
C(2)–M–N(1)	91.08(11)	92.37(10)	91.6(3)	92.28(10)
C(2)–M–N(2)	176.40(19)	178.40(10)	174.6(2)	179.08(14)
C(2)–M–N(3)	91.28(11)	91.76(11)	90.6(3)	–
C(3)–M–N(1)	91.98(11)	90.23(10)	92.1(3)	–
C(3)–M–N(2)	91.88(11)	91.57(10)	92.0(3)	–
C(3)–M–N(3)	177.58(11)	175.23(11)	176.6(3)	–

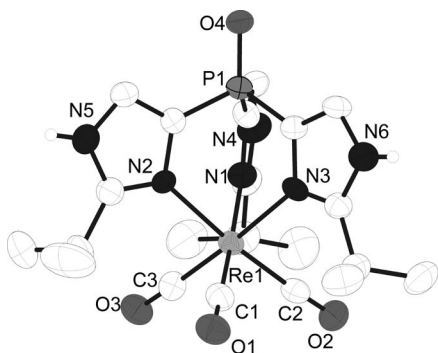


Figure 3. Solid-state structure of **4a**·H₂O·(CH₃)₂CO. Both solvate molecules, the counterion, and nonacidic H atoms are omitted for clarity. Displacement ellipsoids are drawn at the 50% level.

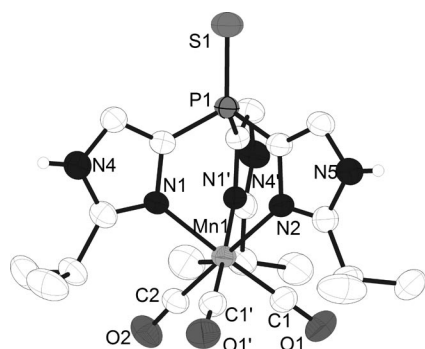


Figure 4. Solid-state structure of **5b**·(C₂H₅)₂O. The diethyl ether solvate molecule, the counterion, and nonacidic H atoms are omitted for clarity. Displacement ellipsoids are drawn at the 50% level.

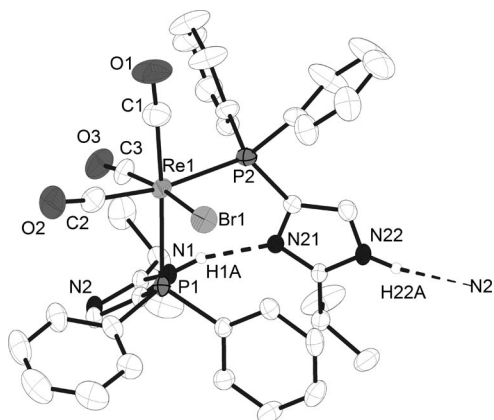


Figure 5. Solid-state structure of **6**. Intra- and intermolecular H-bonds are indicated by dashed lines and nonacidic H-atoms are omitted for clarity. Br(1) and C(3)O(3) show a positional disorder; only one orientation is shown. Displacement ellipsoids are drawn at the 50% level. Selected bond lengths [Å] and angles [°]: Re(1)–P(1) 2.4896(8), Re(1)–P(2) 2.5170(9), Re(1)–Br(1) 2.6169(8), Re(1)–Br(1B) 2.563(2), Re(1)–C(1) 1.934(4), Re(1)–C(2) 1.933(4), Re(1)–C(3) 1.911(7), Re(1)–C(3B) 1.919(14), C(1)–O(1) 1.144(5), C(2)–O(2) 1.149(5), C(3)–O(3) 1.183(8), C(3B)–O(3B) 1.172(16); P(1)–Re(1)–Br(1) 86.98(3), P(1)–Re(1)–Br(1B) 89.49(6), P(2)–Re(1)–Br(1) 99.37(3), P(2)–Re(1)–Br(1B) 90.98(5), P(1)–Re(1)–P(2) 99.67(3), C(2)–Re(1)–C(1) 85.35(18), C(3)–Re(1)–C(1) 94.0(2), C(3B)–Re(1)–P(1) 88.3(4), C(3)–Re(1)–C(2) 90.8(2), C(3B)–Re(1)–C(2) 87.9(5).

rus atoms, and the sixth position in the distorted octahedral environment is occupied by the bromido ligand (Figure 5). In contrast, the imidazolyl N-atoms are not coordinated to the metal center. The positions of the bromido ligand and the carbonyl ligand C(3)O(3) in *trans* position are disordered with an occupancy of 70:30. As shown in Figure 5, the NH functionalities of both imidazolyl rings form intra- and intermolecular hydrogen bonds in the solid state.

Partition Coefficient and CO Release Study

The distribution of drugs in different organs and tissues is mainly determined by the lipophilic/hydrophilic nature of these compounds. Thus, the *n*-octanol/water partition coefficient $\log D$ was determined at pH = 7.4 by the “shake-flask” method to assess the bioavailability of complexes **1–6** (Table 3).^[43] Compared to cisplatin, for which $\log D_{7.4} = -2.53 \pm 0.28$ was determined,^[44] all of the new complexes are more lipophilic, whereas no trend can be recognized in relation to the substitution pattern of the ligands. However, we observed an unexpected reversal of hydrophilicity between the 2-TIP^H and 2-TIP^{NMe} complexes.

Table 3. *n*-Octanol/water partition coefficient $\log D_{7.4}$ of compounds **1–6**, amount of ligand exchange after 24 h in competition with HisOMe, and number of CO equiv. released per mol of complex.

Complex	$\log D_{7.4}$	Ligand exchange	<i>n</i> (CO) released
1a	1.59 ± 0.06	not observed	n.d. ^[a]
2a	0.46 ± 0.02	not observed	n.d.
3a	1.34 ± 0.04	not observed	n.d.
4a	1.86 ± 0.10	not observed	n.d.
1b	0.79 ± 0.03	n.d.	1.82 ± 0.05
2b	−0.16 ± 0.02	4.5%	1.83 ± 0.26
3b	1.48 ± 0.06	21.9%	0.83 ± 0.09
4b	1.27 ± 0.04	n.d.	0.96 ± 0.01
5b	2.02 ± 0.12	23.1%	1.32 ± 0.21
6	1.35 ± 0.03	n.d.	n.d.

[a] n.d.: not determined.

Another critical requirement for compounds intended for use in diagnostic and/or therapeutic applications is the inertness under physiological conditions. In particular, the heavier group 7 transition metal isotopes ^{99m}Tc and ^{186/188}Re can be used for imaging and therapeutic purposes, respectively, because of their favorable nuclear properties (^{99m}Tc: $t_{1/2} = 6$ h, $E_\gamma = 140$ keV; ¹⁸⁸Re: $t_{1/2} = 19.6$ h, $E_\gamma = 2.1$ MeV; ¹⁸⁶Re: $t_{1/2} = 88.9$ h, $E_\gamma = 1.09$ MeV).^[45] Typically, ^{99m}Tc radiopharmaceuticals clear the body within 24 h. In order to mimic the physiological challenges under such conditions, compounds **1a–5a**, **2b**, **3b**, and **5b** were incubated at 1 mM with a 10 mM solution of histidine methyl ester (HisOMe) in [D₆]dmsO for 24 h and spectral changes monitored by ¹H and ³¹P{¹H} NMR spectroscopy. No ligand exchange could be observed in these experiments for the carbonylrhenium compounds **1a–4a**, which highlights the promising properties of these compounds for the development of M(CO)₃-based radiopharmaceuticals. The corresponding manganese compounds are not as inert as the rhenium analogues. After 2 h, a new signal is observed in the

$^{31}\text{P}\{^1\text{H}\}$ spectra of **2b**, **3b**, and **5b**, and after 24 h about 5% of the 2-TIP^{NMe} complex **2b** and 20–25% of the 4-TIP^{iPr} and 4-TIPS^{iPr} complexes **3b** and **5b** have decomposed.

To study the suitability of the compounds to act as novel CO-releasing molecules (CORMs), the manganese complexes **1b–5b** of the general formula $[\text{LMn}(\text{CO})_3]^+$ ($\text{L} = 4\text{-TIPO}^{\text{iPr}}$, $4\text{-TIPS}^{\text{iPr}}$, $4\text{-TIP}^{\text{iPr}}$, and $2\text{-TIP}^{\text{NMe}}$) were investigated by using the UV/Vis-based myoglobin (Mb) assay.^[14] The rhenium complexes do not show any significant absorption above 320 nm and are thus not suitable as photoactivatable CORMs. Changes in the UV/Vis spectra of reduced MbFe^{II} in phosphate buffer in the presence of the metal complexes with and without irradiation at 365 nm were monitored for an extended period of time. In the absence of light, no spectral changes were observed over 1 to 2 h, indicating that complexes **1b–5b** do not release CO spontaneously in aqueous solution in the dark. In contrast, Figure 6 shows the evolution of the spectral features of a mixture of reduced MbFe^{II} in PBS buffer after addition of $[(2\text{-TIP}^{\text{NMe}})\text{Mn}(\text{CO})_3]\text{OTf}$ (**2b**) and subsequent irradiation at 365 nm. The intensity of the Q-band of MbFe at 557 nm slowly decreases, while the typical signature of the MbFeCO adduct appears at 540 and 577 nm. The concentration of MbFeCO can be determined from the absorption data by using $\epsilon_{540\text{ nm}}(\text{MbFeCO}) = 15.4\text{ mmol}^{-1}\text{ L cm}^{-1}$ and applying Lambert-Beer's law. Figure 7 shows the change in absorption at different wavelengths as a function of the irradiation time. Under the conditions employed, photolytic CO release is complete after about 60 min, when all of the complex has been decomposed, as myoglobin was used in excess. In Table 3, the number of CO equiv. released per mol of complex is shown. Interestingly, the substitution pattern of the imidazolyl ligand seems to determine the number of CO equiv. released per mol of complex. Whereas compounds **1b** and **2b** with the imidazol-2-ylphosphane ligand liberate approximately 2 mol of CO per mol of complex, in **3b–5b** with the coordinated imidazol-4-ylphosphanes, only one molecule of CO per $\text{Mn}(\text{CO})_3$ unit is re-

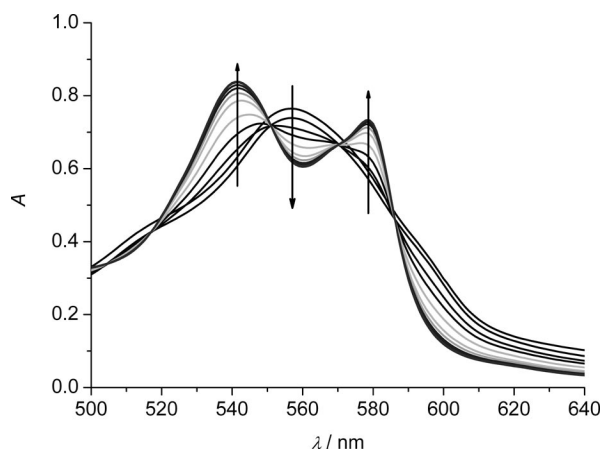


Figure 6. UV/Vis spectral changes in the Q-band region of a solution of reduced horse skeletal muscle myoglobin ($70\text{ }\mu\text{M}$) and $[(2\text{-TIP}^{\text{NMe}})\text{Mn}(\text{CO})_3]\text{OTf}$ (**2b**, $20\text{ }\mu\text{M}$) in 0.1 M phosphate buffer upon irradiation at 365 nm ($t = 0\text{--}150\text{ min}$).

leased, which is also usually found in other complexes $\text{LMn}(\text{CO})_3$.^[46,47] Apparently, the intermediates formed after liberation of the first carbon monoxide have a different reactivity towards further photolytic release of the remaining CO ligands depending on the TIP ligand. The electronic and steric effects that govern this behavior will be the subject of a more detailed study involving time-resolved spectroscopic investigation of **1b–5b** and electronic structure calculations on the title compounds and their photoproducts.

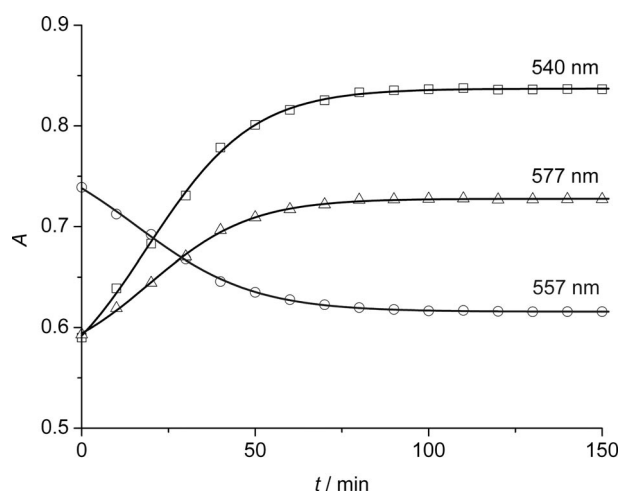


Figure 7. Change of absorption at 540, 557, and 577 nm with time upon radiation at 365 nm of a solution of reduced horse skeletal muscle myoglobin ($70\text{ }\mu\text{M}$) and $[(2\text{-TIP}^{\text{NMe}})\text{Mn}(\text{CO})_3]\text{OTf}$ (**2b**, $20\text{ }\mu\text{M}$) in 0.1 M phosphate buffer.

Conclusions

Ten new Re- and $\text{Mn}(\text{CO})_3$ complexes with imidazolylphosphane ligands have been prepared and fully characterized, including X-ray structure analysis for a number of compounds. In the case of the $\text{P}=\text{E}$ complexes with $\text{E} = \text{O}$ or S , exclusive N,N,N -coordination of the tripodal ligands was observed, whereas if only P - and N -coordination can compete, the former is preferred. The Re complexes of the tripodal ligands were inert towards ligand exchange with histidine in a challenge experiment and all complexes displayed $\log D$ values at physiological pH, which indicated potentially good bioavailability. CO-release investigations of the Mn complexes with the myoglobin assay show that these complexes act as photoinducible CO-releasing molecules (CORMs) upon UV radiation, while they are stable towards decomposition and do not liberate CO spontaneously in the absence of light, even in aqueous solution. The substitution pattern of the imidazolylphosphane ligand was found to determine the number of CO molecules released. Whereas the compounds with the imidazol-2-ylphosphane liberate approximately 2 mol of CO per mol of complex, those with the imidazol-4-ylphosphane release only 1 mol of CO per $\text{Mn}(\text{CO})_3$ unit. Further work will be directed towards additional functionalization of these ligands, for example by conjugation to biomolecules or macromolecular

delivery systems as well as the modification of the tris(imidazolyl)phosphane ligands to alter the CO liberation characteristics. Also, a detailed time-resolved spectroscopic and theoretical study of the primary photoproducts will be carried out to elucidate the factors that govern the different CO release properties.

Experimental Section

General: All reactions were carried out in Schlenk tubes under dry nitrogen by using anhydrous solvents purified according to standard procedures. The metal complexes could be prepared by using nondried solvents. All chemicals were purchased from commercial sources and used as received. ¹H and ³¹P NMR spectra were recorded with a Bruker DRX 200 spectrometer. The ¹H NMR spectra were calibrated against the residual proton signal of the solvent as an internal reference ([D₁]chloroform: δ_H = 7.30 ppm; [D₄]methanol: δ_H = 5.84 ppm; [D₆]acetone: δ_H = 2.05 ppm), whereas the ³¹P{¹H} NMR spectra were referenced to external 85% H₃PO₄. The ESI mass spectra were recorded with a Finnigan LCQ Deca ion trap API mass spectrometer. The MALDI mass spectra were recorded with a Bruker Ultraflex MALDI-TOF mass spectrometer. The FAB mass spectra were recorded with a Finnigan MAT 8200 mass spectrometer by using a nitrobenzyl alcohol (NBA) matrix. Infrared spectra were recorded with a Bruker IFS 66 FTIR spectrometer. The elemental composition of the compounds was determined with a Perkin–Elmer Analysator 2400 at the Institut für Pharmazeutische und Medizinische Chemie, Heinrich-Heine Universität Düsseldorf.

4-TIPSP^{Pr}: In a 100-mL Schlenk flask, 4-TIPSP^{Pr} (500 mg, 1.39 mmol) was dissolved in ethanol (10 mL). Elemental sulfur (134 mg, 4.18 mmol) was added to this solution and the reaction mixture stirred at ambient temperature overnight. The resulting white suspension was filtered, and the white solid that precipitated was washed with carbon disulfide and diethyl ether and then dried in vacuo. Yield 0.46 g (85%). ¹H NMR (200 MHz, [D₄]methanol): δ = 1.33 [d, *J* = 7.0 Hz, 18 H, CH(CH₃)₂], 3.13 [sept, *J* = 7.0 Hz, 3 H, CH(CH₃)₂], 7.42 (d, *J*_{PH} = 2.0 Hz, 3 H, H_{im}) ppm. ³¹P{¹H} NMR (81 MHz, [D₄]methanol): δ = 1.0 (s) ppm. FAB⁺-MS (NBA): *m/z* (%) = 390 (731) [M]⁺, 249 (100) [M – S-im^{Pr}]⁺. C₁₈H₂₇N₆PS·0.5H₂O (399.50): calcd. C 54.41, H 7.06, N 21.04; found C 54.60, H 7.28, N 20.90.

[(2-TIP^H)Re(CO)₃]Br (1a): In a Schlenk tube, 2-TIP^H (58 mg, 0.25 mmol) and [Re(H₂O)₃(CO)₃]Br (100 mg, 0.25 mmol) were dissolved in methanol (20 mL). The solution was stirred at reflux for 5 h. Then the solution was concentrated to 3 mL, and water (20 mL) was added. The precipitated white solid was filtered off and washed with water. The residue was redissolved in methanol, precipitated with *n*-hexane and dried in vacuo to obtain the product as a white solid. Yield 93 mg (144 mg) (65%). ¹H NMR (200 MHz, [D₄]methanol): δ = 7.22 (dd, *J* = 1.0, *J* = 2.7 Hz, 3 H, H_{im}), 7.58 (d, *J* = 1.0 Hz, 3 H, H_{im}) ppm. ³¹P{¹H} NMR (81 MHz, [D₄]methanol): δ = –99.2 (s) ppm. FAB⁺-MS (NBA): *m/z* (%) = 503 (77) [M]⁺, 475 (10) [M – CO]⁺. C₁₂H₉BrN₆O₃PRE^{–5/3}hexane (725.66): calcd. C 29.55, H 2.77, N 13.25; found C 29.48, H 2.73, N 13.09. IR (KBr): ν̄ = 2025 (s), 1898 (vs) cm^{–1}.

[(2-TIP^{NMe})Re(CO)₃]Br (2a): In a Schlenk tube, 2-TIP^{NMe} (69 mg, 0.25 mmol) and [Re(H₂O)₃(CO)₃]Br (100 mg, 0.25 mmol) were dissolved in methanol (15 mL). The solution was stirred at reflux for 3.5 h and then concentrated to 5 mL. Diethyl ether (25 mL) was added and the suspension stored at 0 °C overnight. The precipi-

tated solid was washed with acetone to yield the product as a white solid. Yield: 129 mg (84%). ¹H NMR (200 MHz, [D₄]methanol): δ = 4.08 (s, 9 H, NCH₃), 7.46 (dd, *J* = 1.0, *J* = 4.0 Hz, 3 H, H_{im}), 7.67 (d, *J* = 1.0 Hz, 3 H, H_{im}) ppm. ³¹P{¹H} NMR (81 MHz, [D₄]methanol): δ = –113.5 (s) ppm. ESI-MS (MeOH): *m/z* (%) = 545 (62) [M]⁺, 535 (57) [M – O – CO]⁺, 517 (16) [M – CO]⁺, 489 (15) [M – 2 CO]⁺, 479 (100) [M – oxide – 3 CO]⁺, 461 (96) [M – 3 CO]⁺. C₁₅H₁₅BrN₆O₃PRE·H₂O (642.42): calcd. C 28.04, H 2.67, N 13.08; found C 27.79, H 2.36, N 12.86. IR (KBr): ν̄ = 2007 (s), 1886 (vs) cm^{–1}.

[(4-TIP^{Pr})Re(CO)₃]Br (3a): In a Schlenk tube, 4-TIP^{Pr} (22 mg, 0.062 mmol) and [Re(H₂O)₃(CO)₃]Br (25 mg, 0.062 mmol) were dissolved in methanol (20 mL). The solution was stirred at reflux for 2 h. After this time, the solvent was evaporated, and the residue was washed with acetone to give a white solid product. Yield: 22 mg (50%). ¹H NMR (200 MHz, [D₄]methanol): δ = 1.42 [d, *J* = 7.0 Hz, 18 H, CH(CH₃)₂], 3.90 [sept, *J* = 7.0 Hz, 3 H, CH(CH₃)₂], 7.62 (d, *J* = 2.0 Hz, 3 H, H_{im}) ppm. ³¹P{¹H} NMR (81 MHz, [D₄]methanol): δ = 101.4 (s) ppm. ESI-MS (MeOH/H₂O): *m/z* (%) = 629.4 (100) [M]⁺, 645.4 (35) [M + O]⁺, 601.4 (34) [M – CO]⁺, 410.3 (56) [M – 2 (C₆N₂H₉)]⁺. C₂₁H₂₇BrN₆O₃PRE·0.5H₂O (717.57): calcd. C 35.15, H 3.93, N 11.71; found C 34.89, H 3.54, N 11.47. IR (KBr): ν̄ = 2021 (s), 1902 (vs) cm^{–1}.

[(4-TIPO^{Pr})Re(CO)₃]Br (4a): [Re(CO)₃(H₂O)₃]Br (50 mg, 0.12 mmol) and 4-TIPO^{Pr} (48 mg, 0.12 mmol) were dissolved in methanol (30 mL) and heated to reflux for 3 h. The reaction mixture was then concentrated to 5 mL, and diethyl ether (30 mL) was added. The suspension was stored at 0 °C overnight. After filtration, the precipitated solid was washed with diethyl ether and dried in vacuo to yield 43 mg (50%) of a white solid. Crystals suitable for X-ray single-crystal analysis were obtained by slow evaporation of a water/acetone solution. ¹H NMR (200 MHz, [D₄]methanol): δ = 1.42 [d, *J* = 7 Hz, 18 H, CH(CH₃)₂], 3.90 [sept, *J* = 7.0 Hz, 3 H, CH(CH₃)₂], 7.62 (d, *J* = 2.0 Hz, 3 H, H_{im}) ppm. ³¹P{¹H} NMR (81 MHz, [D₄]methanol): δ = 3.0 (s) ppm. ESI-MS (MeOH/H₂O): *m/z* (%) = 629.4 (100) [M]⁺, 645.4 (35) [M + O]⁺, 601.4 (34) [M – CO]⁺, 410.3 (56) [M – 2 (C₆N₂H₉)]⁺. C₂₁H₂₇BrN₆O₃PRE·0.5H₂O (717.57): calcd. C 35.15, H 3.93, N 11.71; found C 34.89, H 3.54, N 11.47. IR (KBr): ν̄ = 2021 (s), 1902 (vs) cm^{–1}.

[(4-TIPSP^{Pr})Re(CO)₃]Br (5a): [Re(CO)₃(H₂O)₃]Br (50 mg, 0.12 mmol) and 4-TIPSP^{Pr} (48 mg, 0.12 mmol) were dissolved in methanol (30 mL) and heated to reflux for 2 h. The reaction mixture was concentrated to 5 mL, and diethyl ether (30 mL) was added. The suspension was stored at 0 °C overnight. After filtration, the solid was washed with diethyl ether and dried in vacuo. The product still contained a small amount of 4a, as determined by NMR spectroscopy. Yield: 35 mg (39%). ¹H NMR (200 MHz, [D₆]dmsO): δ = 1.31 [d, *J* = 7.0 Hz, 6 H, CH(CH₃)₂], 1.38 [d, *J* = 7.0 Hz, 6 H, CH(CH₃)₂], 1.43 [d, *J* = 7.0 Hz, 6 H, CH(CH₃)₂], 7.97 (s, 2 H, H_{im}), 8.70 (d, *J* = 2.5 Hz, 1 H, H_{im}), 13.37 (br. s, 1 H, NH), 13.71, (br. s, 2 H, NH) ppm. ³¹P{¹H} NMR (81 MHz, [D₆]dmsO): δ = –3.4 (s) ppm. ESI-MS (CH₃OH/HCOOH): *m/z* (%) = 661.4 (100) [(4-TIPSP^{Pr})Re(CO)₃]⁺, 645.4 (20) [(4-TIPO^{Pr})Re(CO)₃]⁺, 603.4 (28) [(4-TIPSP^{Pr})Re(CO)]⁺. IR (KBr): ν̄ = 2029 (s), 1908 (vs) cm^{–1}.

Synthesis of [LMn(CO)₃]OTf Complexes 1b–5b: In a Schlenk tube, pentacarbonylmanganese bromide (100 mg, 0.36 mmol) and silver triflate (93.5 mg, 0.36 mmol) were dissolved in anhydrous acetone (20 mL). After heating to reflux for 1.5 h, the precipitated silver bromide was filtered off and the clear yellow solution added to an acetone solution of the respective ligand (0.36 mmol). Further

heating to reflux for 1.5 h led to formation of the product, which either precipitated directly from the reaction solution (7) or precipitated after reducing the volume of the reaction solution to 5 mL and adding diethyl ether. After filtration, the solid product was washed with diethyl ether and dried in vacuo.

[(2-TIP^H)Mn(CO)₃OTf (1b): Yield: 84 mg (42%). ¹H NMR (200 MHz, [D₄]methanol): δ = 7.32 (br. s, 3 H, H_{im}), 7.68 (br. s, 3 H, H_{im}) ppm. ³¹P{¹H} NMR (81 MHz, [D₄]methanol): δ = -101.7 ppm. ESI-MS (CH₃OH/H₂O): *m/z* (%) = 371.1 (29) [M]⁺, 315.1 (7) [M - 2 CO]⁺, 287.1 (100) [M - 3 CO]⁺. IR (KBr): ν̄ = 2041 (s), 1915 (vs) cm⁻¹. C₁₃H₉F₃MnN₆O₆PS·H₂O·CH₃OH (567.0): calcd. C 29.49, H 2.65, N 14.74; found C 29.55, H 2.31, N 14.56.

[(2-TIP^{NMe})Mn(CO)₃OTf (2b): Yield: 138 mg (61%). ¹H NMR (200 MHz, [D₄]methanol): δ = 4.01 (s, 9 H, NCH₃), 7.38 (d, *J*_{PH} = 4.0 Hz, 3 H, H_{im}), 7.66 (s, 3 H, H_{im}) ppm. ³¹P{¹H} NMR (81 MHz, [D₄]methanol): δ = -115.7 (s) ppm. ESI-MS (CH₃OH): *m/z* (%) = 401.2 (7) [M - CO + O]⁺, 345.7 (11) [M - 3 CO + O]⁺, 329.2 (100) [M - 3 CO]⁺. C₁₆H₁₅F₃MnN₆O₆PS·H₂O (580.3): calcd. C 33.12, H 2.95, N 14.48; found C 33.55, H 2.70, N 14.67. IR (KBr): ν̄ = 2033 (s), 1919 (vs) cm⁻¹.

[(4-TIP^{Pr})Mn(CO)₃OTf (3b): Yield: 197 mg (84%). ¹H NMR (200 MHz, [D₄]methanol): δ = 1.44 [d, *J* = 7.0 Hz, 18 H, CH(CH₃)₂], 3.91 [sept, *J* = 7.0 Hz, 3 H, CH(CH₃)₂], 7.55 (d, *J* = 2.0 Hz, 3 H, H_{im}) ppm. ³¹P{¹H} NMR (81 MHz, [D₄]methanol): δ = -103.6 (s) ppm. ESI-MS (CH₃OH): *m/z* (%) = 497.2 (5) [M]⁺, 441.3 (4) [M - 2 CO]⁺, 413.3 (100) [M - 3 CO]⁺. C₂₂H₂₇F₃MnN₆O₆PS (646.5): calcd. C 40.87, H 4.21, N 13.00; found C 40.94, H 4.38, N 12.77. IR (KBr): ν̄ = 2027 (s), 1933 (vs) cm⁻¹.

[(4-TIPO^{Pr})Mn(CO)₃OTf (4b): Yield: 162 mg (67%). ¹H NMR (200 MHz, [D₄]methanol): δ = 1.45 [d, *J* = 7.0 Hz, 18 H, CH(CH₃)₂], 3.87 [sept, *J* = 7.0 Hz, 3 H, CH(CH₃)₂], 7.81 (s, 3 H, H_{im}) ppm. ³¹P{¹H} NMR (81 MHz, [D₄]methanol): δ = 1.3 (s) ppm. ESI-MS (CH₃OH/H₂O): *m/z* (%) = 513.2 (22) [M]⁺, 457.1 (16) [M - 2 CO]⁺, 429.3 (100) [M - 3 CO]⁺. C₂₂H₂₇F₃MnN₆O₇PS·H₂O

(682.6): calcd. C 38.83, H 4.30, N 12.35; found C 38.77, H 4.80, N 12.10. IR (KBr): ν̄ = 2031 (s), 1935 (vs) cm⁻¹.

[(4-TIPS^{Pr})Mn(CO)₃OTf (5b): Crystals were obtained by slow diffusion of diethyl ether into a methanol solution of 5b. Yield: 153 mg (63%). ¹H NMR (200 MHz, [D₆]acetone): δ = 1.43 [d, *J* = 7.0 Hz, 18 H, CH(CH₃)₂], 3.94 [sept, *J* = 7.0 Hz, 3 H, CH(CH₃)₂], 7.90 (s, 3 H, H_{im}) ppm. ³¹P{¹H} NMR (81 MHz, [D₆]acetone): δ = -7.0 (s) ppm. ESI-MS (CH₃OH/H₂O): *m/z* (%) = 529.2 (17) [M]⁺, 473.0 (13) [M - 2 CO]⁺, 445.2 (100) [M - 3 CO]⁺. C₂₂H₂₇F₃MnN₆O₆PS₂·CH₃OH (710.6): calcd. C 38.88, H 4.40, N 11.83; found C 39.34, H 4.26, N 11.82. IR (KBr): ν̄ = 2032 (s), 1929 (vs) cm⁻¹.

[(4-MIP^{Pr})₂BrRe(CO)₃] (6): In a Schlenk tube, [Re(H₂O)₃(CO)₃]Br (100 mg, 0.25 mmol) and 4-MIP^{Pr} (146 mg, 0.5 mmol) were dissolved in methanol (20 mL). The solution was stirred at reflux for 3 h. The reaction mixture was then concentrated to 5 mL, and, after 48 h at ambient temperature, a colorless solid had precipitated. This was filtered off and washed with methanol to afford a white solid product. Yield: 53 mg (23%). ¹H NMR (200 MHz, [D₁]chloroform): δ = 1.32 [d, *J* = 7.0 Hz, 12 H, CH(CH₃)₂], 2.99 [sept, *J* = 7.0 Hz, 2 H, CH(CH₃)₂], 6.55 (d, *J* = 1.0 Hz, 2 H, H_{im}), 7.27 (m, 20 H, Ph), 11.06 (s, 2 H, NH) ppm. ³¹P{¹H} NMR (81 MHz, [D₁]chloroform): δ = -16.0 ppm. MALDI-MS (CHCl₃): *m/z* (%) = 911.2 (76) [M - CO + H]⁺, 882.2 (51) [M - 2 CO + H]⁺, 859.3 (60) [M - Br]⁺, 831.3 (100) [M - CO - Br]⁺. FAB⁺-MS (NBA): *m/z* (%) = 859.4 (73) [M - Br]⁺, 831.4 (36) [M - CO - Br]⁺, 802.3 (3.3) [M - 2 CO - Br]⁺, 565.1 (22) [M - (4-MIP^{Pr}) - Br]⁺, 509.2 (19) [M - (4-MIP^{Pr}) - CO - Br]⁺. C₃₉H₃₈BrN₄O₃P₂Re (938.81): calcd. C 49.9, H 4.08, N 5.97; found C 49.55, H 3.87, N 5.92. IR (KBr): ν̄ = 2031, 1948, 1920 cm⁻¹.

Partition Coefficients (log *D*): The *n*-octanol/water partition coefficient of compounds 1–6 was determined by using the shake-flask method. PBS-buffered bidistilled water [100 mL, phosphate buffer, *c*(PO₄³⁻) = 10 mM, *c*(NaCl) = 15 mM, pH adjusted to 7.4 with hydrochloric acid] and *n*-octanol (100 mL) were shaken together by using

Table 4. Crystallographic data of 2b, 2b·(CH₃)₂CO, 4a·H₂O·(CH₃)₂CO, 5b·Et₂O, and 6.

	2b	2b·(CH ₃) ₂ CO	4a·H ₂ O·(CH ₃) ₂ CO	5b·Et ₂ O	6
Empirical formula	C ₁₆ H ₁₃ F ₃ MnN ₆ O ₆ PS	C ₁₉ H ₂₁ F ₃ MnN ₆ O ₇ PS	C ₂₅ H ₃₅ F ₃ N ₆ O ₉ PReS	C ₂₆ H ₃₇ F ₃ MnN ₆ O ₇ PS ₂	C ₃₉ H ₃₈ BrN ₄ O ₃ P ₂ Re
<i>M</i> [g mol ⁻¹]	562.31	620.39	869.82	752.65	938.78
Diffractionmeter	Oxford Excalibur, Ruby CCD detector	Oxford Excalibur, Ruby CCD detector	Stoe IPDS	Stoe IPDS	Oxford Excalibur, Ruby CCD detector
<i>T</i> [K]	183(2)	183(2)	183(2)	183(2)	183(2)
Crystal system	monoclinic	triclinic	triclinic	orthorhombic	monoclinic
Space group	<i>P</i> 2 ₁ / <i>c</i>	<i>P</i> $\bar{1}$	<i>P</i> $\bar{1}$	<i>Pnma</i>	<i>P</i> 2 ₁ / <i>c</i>
<i>a</i> [Å]	10.4537(4)	8.0165(3)	9.6736(9)	17.1900(8)	9.58994(6)
<i>b</i> [Å]	13.1812(5)	11.7299(6)	12.2041(11)	12.7363(7)	19.50377(11)
<i>c</i> [Å]	16.0452(7)	14.9909(6)	16.3861(13)	16.0560(7)	20.82476(13)
<i>a</i> [°]		86.923(4)	76.03(1)		
<i>β</i> [°]	92.067(3)	79.851(4)	76.10(1)		96.2878(6)
<i>γ</i> [°]		74.991(4)	69.73(1)		
<i>V</i> [Å ³]	2209.47(15)	1340.1(1)	1734.7(3)	3515.3(3)	3871.63(4)
<i>Z</i>	4	2	2	4	4
<i>D</i> _{calcd.} [Mg m ⁻³]	1.690	1.537	1.665	1.422	1.611
<i>μ</i> /mm ⁻¹	0.837	0.700	3.680	0.605	4.295
Reflections collected	21758	13206	20765	31823	118629
Independent reflections	6729 [0.0439]	6656 [0.0380]	7129 [0.0803]	4208 [0.1016]	11815 [0.0357]
[<i>R</i> _{int}]					
Final <i>R</i> indices [<i>I</i> > 2σ(<i>I</i>)]	<i>R</i> ₁ = 0.0522 <i>wR</i> ₂ = 0.1157	<i>R</i> ₁ = 0.0444 <i>wR</i> ₂ = 0.0662	<i>R</i> ₁ = 0.0611 <i>wR</i> ₂ = 0.1484	<i>R</i> ₁ = 0.0587 <i>wR</i> ₂ = 0.1460	<i>R</i> ₁ = 0.0324 <i>wR</i> ₂ = 0.0752
Final <i>R</i> indices (all data)	<i>R</i> ₁ = 0.0948 <i>wR</i> ₂ = 0.1228	<i>R</i> ₁ = 0.1098 <i>wR</i> ₂ = 0.0736	<i>R</i> ₁ = 0.0697 <i>wR</i> ₂ = 0.1545	<i>R</i> ₁ = 0.0735 <i>wR</i> ₂ = 0.1545	<i>R</i> ₁ = 0.0439 <i>wR</i> ₂ = 0.0774

a laboratory shaker (Perkin–Elmer) for 72 h to allow saturation of both phases. Each compound (1 mg) was mixed in aqueous and organic phase (1 mL) for 10 min by using a laboratory vortexer. The resulting emulsion was centrifuged (3000 g, 5 min) to separate the phases. The concentrations of each complex in the aqueous and organic phases were determined by using UV/Vis spectroscopy at 260 nm; $\log D_{\text{pH}}$ was defined as the logarithm of the ratio of the concentrations of the complex in the organic and aqueous phase ($\log D = \log \{[\text{complex}_{(\text{org})}]/[\text{complex}_{(\text{aq})}]\}$); the value reported is the mean of three separate determinations.

CO-Release Studies: All UV/Vis measurements were performed with a Jasco V-670 spectrophotometer at room temperature in a quartz cuvette ($d = 1$ cm). Horse skeletal muscle myoglobin (Fluka) was dissolved in 0.1 M phosphate buffer pH = 7.3 and degassed by bubbling with nitrogen. Then, it was reduced by the addition of an excess of sodium dithionite in the same solvent, and finally buffer was added to the cuvette to a total volume of 749 μL . To this solution, complex (1 μL) dissolved in dimethyl sulfoxide was added to give a final concentration of 20 $\mu\text{mol L}^{-1}$ of metal complex and 75 $\mu\text{mol L}^{-1}$ of myoglobin with $A(557 \text{ nm}) < 1$. Solutions were then either kept in the dark or irradiated for given time intervals under nitrogen at 365 nm with a UV hand lamp positioned perpendicular to the cuvette at a distance of 6 cm. Irradiations were interrupted at regular intervals to take UV/Vis spectra. All measurements were carried out in triplicate to analyze the reproducibility of the CO release.

Crystallography: Crystallographic data were collected at 183(2) K with Mo- K_{α} radiation ($\lambda = 0.7107 \text{ \AA}$) that was graphite-monochromated. Suitable crystals were covered with oil (Infinitec V8512, formerly known as Paratone N), mounted on top of a glass fiber, and immediately transferred to the diffractometer. The crystals were measured either with a Stoe IPDS diffractometer [for **4a**·H₂O·(CH₃)₂CO and **5b**·Et₂O] or an Oxford Diffraction Xcalibur system with a Ruby detector [for **2b**, **2b**·(CH₃)₂CO, and **6**] (Table 4). In the case of the IPDS, a maximum of 8000 reflections distributed over the whole limiting sphere were selected by the program SELECT and used for unit-cell parameter refinement with the program CELL.^[48] Data were corrected for Lorentz and polarization effects as well as for absorption (numerical). In the case of the Oxford system, the program suite CrysAlis^{Pro} was used for data collection, semiempirical absorption correction, and data reduction.^[49] Structures were solved with direct methods by using SIR97^[50] and were refined by full-matrix least-squares methods on F^2 with SHELXL-97.^[51] The structures were checked for higher symmetry with the help of the program Platon.^[52] CCDC-739736, -739737, -739738, -739739, and -739740 contain the supplementary crystallographic data for this paper. These data can be obtained free of charge from The Cambridge Crystallographic Data Centre via www.ccdc.cam.ac.uk/data_request/cif.

Supporting Information (see footnote on the first page of this article): Details on crystal data and structure refinement for **2b**, **4a**, **5b**, and **6**; picture of the solid-state structure of **2b**·(CH₃)₂CO.

Acknowledgments

Part of this work was supported by the Deutsche Forschungsgemeinschaft (DFG) within FOR 630 (“Biological function of organometallic compounds”) and the Fonds der Chemischen Industrie (FCI). A. R. thanks the Deutscher Akademischer Austauschdienst (DAAD) for an International Association for the Exchange of Students for Technical Experience (IAESTE) fellowship. U. S. thanks

Prof. Dr. Nils Metzler-Nolte and P. C. K. thanks Prof. Dr. Wolfgang Kläui for generous access to all facilities of the institutes.

- [1] B. E. Mann, R. Motterlini, *Chem. Commun.* **2007**, 4197.
- [2] L. Wu, R. Wang, *Pharmacol. Rev.* **2005**, *57*, 585.
- [3] S. W. Ryter, J. Alam, A. M. K. Choi, *Physiol. Rev.* **2006**, *86*, 583.
- [4] M. Vadori, M. Seveso, F. Besenzone, E. Bosio, E. Tognato, F. Fante, M. Boldrin, S. Gavasso, L. Ravarotto, B. Mann, P. Simioni, E. Ancona, R. Motterlini, E. Cozzi, *Xenotransplantation* **2009**, *16*, 99.
- [5] E. Stagni, M. Privitera, C. Bucolo, G. Leggio, R. Motterlini, F. Drago, *Br. J. Ophthalmol.* **2009**, *93*, 254.
- [6] S. Chlopicki, R. Olszanecki, E. Marcinkiewicz, M. Lomnicka, R. Motterlini, *Cardiovasc. Res.* **2006**, *71*, 393.
- [7] R. Alberto, R. Motterlini, *Dalton Trans.* **2007**, 1651.
- [8] T. R. Johnson, B. E. Mann, R. Foresti, R. Motterlini, *Circ. Res.* **2003**, *42*, 3722.
- [9] R. Motterlini, B. E. Mann, R. Foresti, *Expert Opin. Invest. Drugs* **2005**, *14*, 1305.
- [10] J. E. Clark, P. Naughton, S. Shurey, C. J. Green, T. R. Johnson, B. E. Mann, R. Foresti, R. Motterlini, *Circ. Res.* **2003**, *93*, e2.
- [11] I. J. S. Fairlamb, J. M. Lynam, B. E. Moulton, I. E. Taylor, A. K. Duhme-Klair, P. Sawle, R. Motterlini, *Dalton Trans.* **2007**, 3603.
- [12] P. Sawle, J. Hammad, I. J. S. Fairlamb, B. Moulton, C. T. O'Brien, J. M. Lynam, A. K. Duhme-Klair, R. Foresti, R. Motterlini, *J. Pharmacol. Exp. Ther.* **2006**, *318*, 403.
- [13] I. J. S. Fairlamb, A.-K. Duhme-Klair, J. M. Lynam, B. E. Moulton, C. T. O'Brien, P. Sawle, J. Hammad, R. Motterlini, *Bioorg. Med. Chem. Lett.* **2006**, *16*, 995.
- [14] R. Motterlini, J. E. Clark, R. Foresti, P. Sarathchandra, B. E. Mann, C. J. Green, *Circ. Res.* **2002**, *90*, e17.
- [15] J. Niesel, A. Pinto, H. W. Peindy N'Dongo, K. Merz, I. Ott, R. Gust, U. Schatzschneider, *Chem. Commun.* **2008**, 4292.
- [16] H. Pfeiffer, A. Rojas, J. Niesel, U. Schatzschneider, *Dalton Trans.* **2009**, 4292.
- [17] W. Zhang, A. Atkin, R. Thatcher, A. Whitwood, I. Fairlamb, J. Lynam, *Dalton Trans.* **2009**, 4351.
- [18] A. Atkin, S. Williams, P. Sawle, R. Motterlini, J. Lynam, I. Fairlamb, *Dalton Trans.* **2009**, 3653.
- [19] S. Trofimenko, *Polyhedron* **2004**, *23*, 197.
- [20] S. Trofimenko, *Scorpionates: The Coordination Chemistry of Polypyrazolylborate Ligands*, Imperial College Press, London, **1999**.
- [21] C. Pettinari, *Scorpionates II: Chelating Borate Ligands*, Imperial College Press, London, **2008**.
- [22] P. C. Kunz, W. Kläui, *Collect. Czech. Chem. Commun.* **2007**, *72*, 492.
- [23] P. Kunz, G. Reiß, W. Frank, W. Kläui, *Eur. J. Inorg. Chem.* **2003**, 3945.
- [24] F. J. Wu, D. M. Kurtz Jr, K. S. Hagen, P. D. Nyman, *Inorg. Chem.* **1990**, *29*, 5174.
- [25] N. J. Curtis, R. S. Brown, *J. Org. Chem.* **1980**, *45*, 4038.
- [26] P. C. Kunz, M. U. Kassack, A. Hamacher, B. Spingler, *Dalton Trans.* **2009**, 7741.
- [27] N. Lazarova, S. James, J. W. Babich, J. Zubieta, *Inorg. Chem. Commun.* **2004**, *7*, 1023.
- [28] J. A. Casares, P. Espinet, R. Hernando, G. Iturbe, F. Villafane, D. J. Ellis, A. G. Orpen, *Inorg. Chem.* **1997**, *36*, 44.
- [29] R. Raturi, J. Lefebvre, D. B. Leznoff, B. R. McGarvey, S. A. Johnson, *Chem. Eur. J.* **2008**, *14*, 721.
- [30] H. Han, S. A. Johnson, *Eur. J. Inorg. Chem.* **2008**, 471.
- [31] H. Han, S. A. Johnson, *Organometallics* **2006**, *25*, 5594.
- [32] H. Han, M. Elsmaili, S. A. Johnson, *Inorg. Chem.* **2006**, *45*, 7435.
- [33] P. S. Braterman, *Metal Carbonyl Spectra*, Academic Press, London, **1975**.
- [34] D. L. Reger, J. R. Gardinier, S. Bakbak, R. F. Semeniuc, U. H. F. Bunz, M. D. Smith, *New J. Chem.* **2005**, *29*, 1035.

- [35] D. L. Reger, R. F. Semeniuc, M. D. Smith, *J. Organomet. Chem.* **2003**, 666, 87.
- [36] D. L. Reger, T. C. Grattan, *Synthesis* **2003**, 960.
- [37] D. L. Reger, R. F. Semeniuc, M. D. Smith, *J. Chem. Soc., Dalton Trans.* **2002**, 476.
- [38] D. L. Reger, T. C. Grattan, K. J. Brown, C. A. Little, J. J. S. Lamba, A. L. Rheingold, R. Sommer, *J. Organomet. Chem.* **2000**, 607, 120.
- [39] P. Kunz, M. Berghahn, N. Brückmann, M. Dickmeis, M. Kettel, B. Spingler, *Z. Anorg. Allg. Chem.* **2009**, 635, 471.
- [40] R. S. Herrick, C. J. Ziegler, D. L. Jameson, C. Aquina, *Dalton Trans.* **2008**, 3605.
- [41] P. Kunz, P. Kurz, B. Spingler, R. Alberto, *Acta Crystallogr., Sect. E* **2007**, 63, m363.
- [42] D. L. Reger, K. J. Brown, M. D. Smith, *J. Organomet. Chem.* **2002**, 658, 50.
- [43] B. Faller, F. Wohnsland in *Pharmacokinetic Optimization in Drug Research* (Eds.: B. Testa, H. Van de Waterbeemd, G. Folkers, R. H. Guy), VCH & Wiley-VCH, Zürich, Weinheim, **2001**, p. 257.
- [44] D. Screnci, M. J. McKeage, P. Galettis, T. W. Hambley, *Br. J. Cancer* **2000**, 82, 966.
- [45] K. Schwochau, *Technetium*, Wiley-VCH, Weinheim, **2000**.
- [46] K. Kunz, M. Bolte, H.-W. Lerner, M. Wagner, *Organometallics* **2009**, 28, 3079.
- [47] J. Full, C. Daniel, L. Gonzáles, *Phys. Chem. Chem. Phys.* **2003**, 5, 87.
- [48] STOE & Cie. GmbH, *STOE-IPDS Software Package*, Darmstadt, Germany, **1999**.
- [49] Oxford Diffraction Ltd., *ChrysAlisPro Software System, version 171.32*, Oxford, UK, **2007**.
- [50] A. Altomare, M. C. Burla, M. Camalli, G. L. Cascarano, *J. Appl. Crystallogr.* **1999**, 32, 115.
- [51] G. M. Sheldrick, *Acta Crystallogr., Sect. A* **2008**, 64, 112.
- [52] A. L. Spek, *J. Appl. Crystallogr.* **2003**, 36, 7.

Received: July 10, 2009

Published Online: November 4, 2009